

# Non-linear rate-equilibrium free energy relationships and Hammond behavior in protein folding

Ignacio E. Sánchez, Thomas Kiefhaber\*

*Biozentrum der Universität Basel, Department of Biophysical Chemistry, Klingelbergstrasse 70, CH-4056 Basel, Switzerland*

Received 19 April 2002; accepted 31 May 2002

## Abstract

Non-linear rate-equilibrium relationships upon mutation or changes in solvent conditions are frequently observed in protein folding reactions and are usually interpreted in terms of Hammond behavior. Here we first give a general overview over the concept of transition state movements in chemical reactions and discuss its application to protein folding. We then show examples for genuine Hammond behavior and for apparent transition state movements caused by other effects like changes in the rate-limiting step of the folding reaction or ground state effects, i.e. structural changes in either the native state or the unfolded state. These examples show that apparent transition state movements can easily be mistaken for Hammond behavior. We describe experimental tests using self- and cross-interaction parameters to distinguish between structural changes in a single transition state following Hammond behavior and apparent transition state movements caused by other effects.

© 2002 Elsevier Science B.V. All rights reserved.

**Keywords:** Protein folding kinetics; Transition state; Rate-equilibrium relationships; Hammond postulate; Cross-interaction parameters; Folding intermediates

## 1. Free energy relationships and the Hammond postulate

The characterization of the transition state of a reaction is one of the main goals in kinetic studies. One of the oldest approaches to the characterization of transition states is the rate-equilibrium free

energy relationship, formulated in 1953 by Leffler [1]. He observed that in many reactions the changes in activation free energy ( $\Delta G^{\ddagger}$ ) induced by changes in the medium (solvent) or in structure are linearly related to the corresponding changes in equilibrium free energy ( $\Delta G^0$ ) between reactants and products. Leffler defined a proportionality constant,  $\alpha_x$ , which reflects the energetic sensitivity of the transition state relative to that of the ground states in response to a perturbation,  $\partial x$ .

\*Corresponding author. Tel.: +41-61-267-2194, fax: +41-61-267-2189.

E-mail address: t.kiefhaber@unibas.ch (T. Kiefhaber).

$$\alpha_x = \frac{\partial \Delta G^{0\dagger} / \partial x}{\partial \Delta G^0 / \partial x} \quad (1)$$

He postulated that this energetic reaction coordinate could be understood in structural terms. In its original formulation the Leffler postulate was proposed for reactions in organic chemistry, in which only one or two covalent bonds are relevant for the progress of a reaction ('microscopic' reaction coordinates). In this situation, the 'macroscopic'  $\alpha_x$  given by the rate-equilibrium free energy relationship can easily be related to the 'microscopic' one. Free energy relationships of the Leffler type are generally linear over a broad range of equilibrium free energies for the reference reaction (sometimes up to 50 kJ/mol) and for a wide variety of reaction rates and mechanisms [2].

Deviations from linearity in the rate-equilibrium free energy relationship are commonly observed. Four major effects have been described to cause these non-linearities: (i) a change in the rate limiting step, e.g. if the rate constant reaches the diffusion limit, (ii) a change in the mechanism of the reaction (iii) a change in the energetic sensitivity of the transition state relative to the ground states, i.e. a movement of the position of the transition state along the reaction coordinate [3] or (iv) two reaction series with different steric effects are compared. If the rate-limiting step or the mechanism of a reaction changes, a discrete jump in the position of the transition state along the reaction coordinate is observed. A transition state movement will result in a rather smooth structural shift of the position of transition state upon perturbation. Such a transition state movement is related to the Hammond postulate, which states that 'if two states, as for example, a transition state and an unstable intermediate occur consecutively during a reaction process and have nearly the same energy content, their interconversion will involve only a small reorganization of the molecular structures' [4]. In other words, the structure of a transition state should move closer to the structure of that state that is destabilized by the perturbation.

It is worth discussing Thornton's theoretical explanation of transition state movements [5]. It assumes that the transition state is a saddle point

in the energy landscape of the reaction. It is an energy maximum in the direction of the reaction coordinate and an energy minimum in all other directions. A second assumption is that the potential for each vibrational mode of the molecule can be approximated by a quadratic function. The vibration of the reacting bond(s), the one(s) that are formed or broken in the reaction, is considered to be parallel to the reaction coordinate. Since the transition state is located at a maximum of the parabolic potential along the reaction coordinate, it will shift towards the destabilized state if a linear free energy perturbation is applied (Fig. 1a). All other vibrational modes of the molecule are considered to be perpendicular to the reaction coordinate. For those, the transition state is at the minimum of the parabolic potential, which will shift towards the stabilized side of the coordinate if a linear perturbation is applied (Fig. 1b). These are the two 'reacting bond rules' in the IUPAC nomenclature [6], which are sometimes referred to as 'Hammond effect' and 'anti-Hammond effect'. The effect of the perturbation on the structure of the transition state will be the sum of the individual effects on all coordinates. This theory is valid for any transition state along the reaction coordinate and does not require the product to have nearly the same energy content as the transition state. Movements of the transition state are thus expected if the energy landscape around it has a smooth curvature and different regions become limiting after a perturbation (Fig. 2a) [3], e.g. in reactions taking place with a continuum of mechanisms, such as olefin eliminations and nucleophilic substitutions. A perturbation will not yield an observable change in the position of the maximum along the coordinate if the transition state of a reaction is a narrow energy maximum in the reaction coordinate (Fig. 2b).

Since the location of the transition state is a normalized parameter it is always defined relative to the ground states. Consequently, the effect of a perturbation on the structure of the ground states also has to be taken into account in an analysis for Hammond behavior [7]. A change in the structure of one of the ground states of a reaction changes the 'length' of the reaction coordinate. This can lead to an apparent movement of the

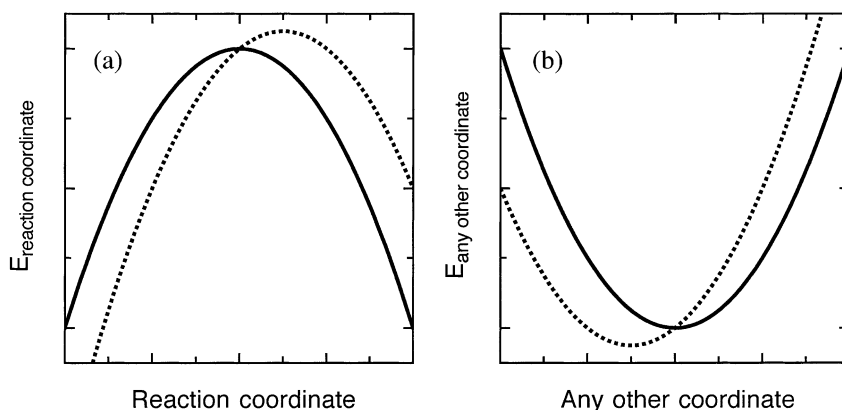


Fig. 1. Illustration of Thornton's first (a) and second reacting bond rules (b). The energy landscape in the vicinity of a transition state is approximated by a parabolic potential, both before (continuous line) and after (dotted line) a linear perturbation. (a) In the direction of the reaction coordinate the transition state is a maximum on the energy landscape, which will shift towards the state that is destabilized (b) In a direction perpendicular to the reaction coordinate the transition state is a minimum on the energy landscape, which will shift towards the state that is stabilized. Adapted from [5].

position of the transition state without a change in its structure (Fig. 3). It is therefore essential to characterize the effect of a perturbation on all states along the reaction coordinate in order to discriminate between ground state effects and transition state movements.

## 2. Self-interaction and cross-interaction parameters

A systematic way to analyze transition state movements was proposed by Jencks and coworkers

[8] by applying self-interaction and cross-interaction parameters. A self-interaction parameter ( $p_x$ ) measures the shift in the position of the transition state along the reaction coordinate due to changes in equilibrium free energy upon perturbation. Such a shift causes a curvature in the corresponding free energy relationship. If we adapt it to Leffler's rate-equilibrium free energy relationship we have

$$p_x = \frac{\partial \alpha_x}{\partial \Delta G_x^0} = \frac{\partial^2 \Delta G^{0\dagger}}{(\partial \Delta G_x^0)^2} \quad (2)$$

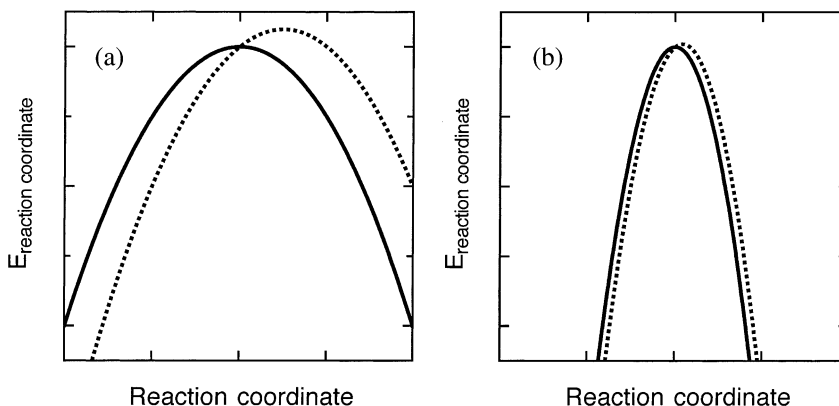


Fig. 2. Response of two parabolic potentials of different curvature to the same linear perturbation. The illustration shows that the position of a transition state in a broad barrier region (a) is more sensitive to the perturbation than in a narrow barrier region (b). Adapted from [3,5].

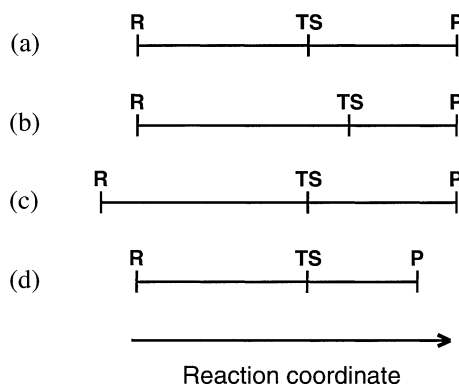


Fig. 3. Schematic representation of transition state movements caused by Hammond behavior (b) and apparent transition state movements relative to the reference reaction coordinate (a) caused by ground state effects due to changes in the structure of the reactants (c) or of the products (d).

By definition a shift in the transition state towards the destabilized state will give a positive  $p_x$ .

Curvatures in free energy relationships are sometimes difficult to evaluate because the energy range of the measurements is too narrow, the curvature too small or the structure/medium perturbations have other, undesired side effects [3]. A way to overcome these problems is the determination of a cross-interaction parameter ( $p_{xy}$ ), which measures a shift in the position of the transition state  $\alpha_x$  (measured by the perturbation  $\partial x$ ) caused by a second perturbation  $\partial y$ .

$$p_{xy} = \frac{\partial \alpha_x}{\partial \Delta G_y^0} = \frac{\partial^2 \Delta G^{0\dagger}}{(\partial \Delta G_x^0)(\partial \Delta G_y^0)} = \frac{\partial \alpha_y}{\partial \Delta G_x^0} = p_{yx} \quad (3)$$

If  $p_{xy}$  is non-zero, a linear free energy relationship caused by  $\partial x$  will have different slopes when measured under different constant amounts of  $\partial y$ . Jencks and coworkers used self- and cross-interaction parameters to calculate the shape of the energy landscape around a transition state, assuming that the transition state is a saddle point in the energy landscape [8].

### 3. Free energy relationships in protein folding

Rate-equilibrium free energy relationships for protein folding reactions can be derived in various

ways. Let us consider the Gibbs fundamental equation

$$d\Delta G^0 = \Delta V^0 dp - \Delta S^0 dT + \sum \Delta \mu_i^0 dn_i \quad (4)$$

where  $\Delta G^0$ ,  $\Delta V^0$ ,  $\Delta S^0$  and  $\sum \Delta \mu_i^0$  are the differences in Gibbs free energy, volume, entropy and chemical potential, respectively, between the unfolded and the native states. If we make use of transition state theory [9,10], the Gibbs equation can be applied to the activation free energy:

$$d\Delta G^{0\dagger} = \Delta V^{0\dagger} dp - \Delta S^{0\dagger} dT + \sum \Delta \mu_i^{0\dagger} dn_i \quad (5)$$

For equilibrium and kinetic measurements at constant temperature and different pressures Lefler's equation can be rewritten as [11]:

$$\alpha_p = \frac{\partial \Delta G^{0\dagger} / \partial p}{\partial \Delta G^0 / \partial p} = \frac{\Delta V^{0\dagger}}{\Delta V^0} \quad (6)$$

For measurements at constant pressure and different temperatures we get:

$$\alpha_T = \frac{\partial \Delta G^{0\dagger} / \partial T}{\partial \Delta G^0 / \partial T} = \frac{\Delta S^{0\dagger}}{\Delta S^0} \quad (7)$$

$\alpha_T$  can be seen as an entropic reaction coordinate [12]. Its value changes with temperature due to the change in heat capacity associated with protein folding reactions [13]. This non-zero  $\Delta C_p^0$  allows the definition of another reaction coordinate [14]

$$\alpha_c = \frac{\Delta C_p^{0\dagger}}{\Delta C_p^0} \quad (8)$$

Eqs. (6)–(8) can be considered as medium-induced rate-equilibrium free energy relationships.

A protein folding equilibrium can also be perturbed by the addition of chemical denaturants, such as urea or guanidinium chloride (GdmCl). In most cases, the equilibrium free energy of the reaction depends linearly on the concentration of the denaturant [15]. The proportionality constant is called the equilibrium  $m$ -value ( $m_{eq}$ ).

$$m_{eq} = \frac{\partial \Delta G^0}{\partial [\text{Denaturant}]} \quad (9)$$

The  $m_{eq}$ -value is empirically found to be proportional to the difference in solvent accessible surface area between the native and unfolded state

[16]. The Gibbs equation can be adapted to include this effect.

$$d\Delta G^0 = \Delta V^0 dp - \Delta S^0 dT + m_{eq} d[\text{Denaturant}] \quad (10)$$

Linear dependencies are also observed for the activation free energies for folding and unfolding [17]. Accordingly, the kinetic  $m$ -values for the folding ( $m_f$ ) and unfolding reactions ( $m_u$ ), can be defined as

$$m_{f,u} = \frac{\partial \Delta G_{f,u}^{0*}}{\partial [\text{Denaturant}]} \quad (11)$$

Thus the activation free energy becomes

$$d\Delta G_{f,u}^{0*} = \Delta V_{f,u}^{0*} dp - \Delta S_{f,u}^{0*} dT + m_{f,u} d[\text{denaturant}] \quad (12)$$

Based on these observations Tanford defined a medium-induced free energy relationship [17].

$$\alpha_D = \frac{\partial \Delta G_f^{0*} / \partial [\text{Denaturant}]}{\partial \Delta G^0 / \partial [\text{Denaturant}]} = \frac{m_f}{m_{eq}} \quad (13)$$

In this case  $\alpha_D$  defines the relative change in solvent accessible surface area between the unfolded state and the transition state.

Other solvent additives such as alcohols (2,2,2-trifluoroethanol), polyols (glycerol, sugars), salts ( $\text{Na}_2\text{SO}_4$ ,  $\text{NaCl}$ ) or  $\text{D}_2\text{O}$  as solvent can also change the stability of a protein proportional to their concentration and can therefore be used to define the corresponding medium-induced  $\alpha$ -value [18]. Changes in solvent viscosity with changes in medium composition and temperature can be considerable and non-additive and should also be taken into account [19,20].

Also structure-induced rate-equilibrium free energy relationships can be obtained for protein folding reactions. This approach was pioneered by Matthews [21] and Fersht [22]. It tests the relative energetic sensitivity of the transition state to stability effects induced by structural changes upon site-directed mutagenesis.

$$\alpha_S = \phi_f = \frac{\partial \Delta G_f^{0*} / \partial \text{Structure}}{\partial \Delta G^0 / \partial \text{Structure}} \quad (14)$$

The term  $\phi_f$  is commonly used in protein folding literature instead of  $\alpha_S$ . The  $\phi_f$ -value reflects the presence of interactions made by the

mutated residue in the transition state with the limiting cases of  $\phi_f = 1$  when the interactions are completely formed and  $\phi_f = 0$  if they are completely absent in the transition state. Usually different parts of the protein are probed to get a picture of the transition state for folding with resolution at the residue level [23]. In most cases only one perturbation is made for each position. This gives a free energy relationship with only two data points and introduces some uncertainty in the results [24]. A recent experimental study compared the effect of eight different amino acid side chains at the same position of an SH3 domain. The results show that the  $\phi_f$ -values range from 0.31 to 0.60 for the different amino acids at this single position [25]. Averaging the data from different positions all over a protein or in a substructure of a protein yields an average  $\phi_f$ -value,  $\langle \phi_f \rangle$ . This parameter is more reliable than individual  $\phi_f$ -values, but of lower resolution [26]. Another possible structure-induced perturbation is the deuteration of backbone hydrogen bonds, which can be used to calculate an  $\alpha_{HD}$  [27].

Ligand binding is another source of changes in protein stability and thus allows characterization of the transition state [17]. Many proteins bind ions, substrates or cofactors, and all bind hydrogen ions at ionizable side chains. The changes in free energy upon binding are proportional to the logarithm of the ligand concentration and can be used to determine an  $\alpha_L$  [28–31], which represents the binding ability of the transition state.

The interpretation of the ‘macroscopic’  $\alpha$  for a protein folding reaction is obviously more complicated than in simple organic reactions. During the folding of a protein many non-covalent protein–protein, protein–solvent and solvent–solvent interactions are formed and broken, even for a single side chain. Therefore, many ‘microscopic’ reaction coordinates may be significant in determining the value of the ‘macroscopic’  $\alpha$ . The interpretation of the  $\alpha$ -values and their changes becomes less straightforward and often relies on empirical relations derived from equilibrium data [16,32]. Also, for the shape of a multidimensional energy landscape more complex scenarios than a saddle point are to be expected, for which the effects on the ‘macroscopic’ reaction coordinates are unknown

[33]. The description of transition states in protein folding therefore requires as much experimental information as possible about different ‘macroscopic’ reaction coordinates and their relation to the ‘microscopic’ ones.

#### 4. Transition state movements in protein folding

The analysis and interpretation of kinetic data in protein folding is most straightforward for two-state folding. In this case a plot of the logarithm of the single observable apparent rate constant,  $\lambda$  ( $\lambda = k_f + k_u$ ) vs. chemical denaturant concentration yields a V-shaped curve, commonly called Chevron plot (Fig. 4a) [21,34]. This plot gives information on the refolding reaction at low denaturant concentrations (the refolding limb) and information on the unfolding reaction at high denaturant concentrations (the unfolding limb). For many two-state folders perfectly linear free energy relationships have been reported up to a 30 kJ/mol range of variation in protein stability ( $p_D = \partial \alpha_D / \partial \Delta G_D^0 = 0$ ) [35,36] suggesting that for those proteins the folding transition states are narrow and robust maxima. For several two-state folders, however, non-linear free energy relationships ( $p_D \neq 0$ ) have been observed without evidence for transiently populated intermediate states. Fersht and coworkers proposed Hammond behavior associated with a broad transition state region [37–41] as origin for these non-linearities (Fig. 5a). This interpretation has since then been commonly used to explain non-linear free energy relationships in protein folding. However, non-linear free energy relationships can also be caused by a change in the rate-limiting step of a reaction as discussed above. Fig. 4b shows the chevron plot of a tendamistat variant that exhibits a non-linear unfolding limb of the chevron plot. At low (<2 M GdmCl) and high denaturant concentrations (>5 M GdmCl), however, the  $\alpha_D$  value is constant indicating a denaturant-induced switch between two distinct transition states [42]. This suggests a sequential folding model with consecutive transition states and a metastable high energy intermediate (Fig. 5b). A recent analysis showed that the sequential model is also able to explain denaturant-induced non-linear activation free energy relation-

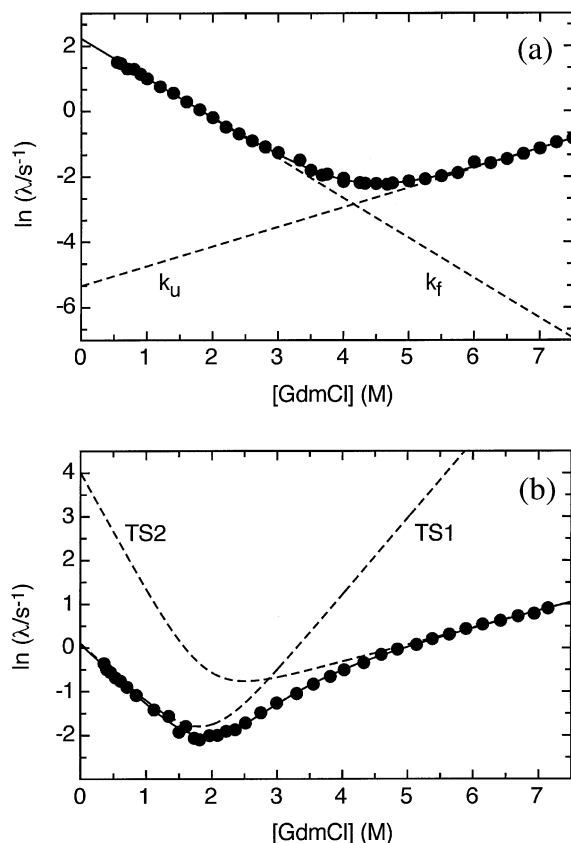


Fig. 4. (a) Plot of  $\ln \lambda$  vs. GdmCl concentration (Chevron plot) for wild-type tendamistat at pH 2 (●). The solid line shows the fit to a two-state model ( $\lambda = k_f + k_u$ ). The dashed lines indicate the GdmCl-dependence of the microscopic rate constants,  $k_f$  and  $k_u$ . Due to the linear dependence of  $\Delta G^0$  on denaturant concentration [15] the linear changes in  $\ln k_u$  and  $\ln k_f$  with denaturant concentration can be considered as linear rate-equilibrium free energy relationships. (b) Curved Chevron plot for the C45AC73A variant of tendamistat (●). The linear dependence of  $\ln \lambda$  on denaturant concentration above and below the curved region indicates a shift between 2 distinct transition states [42]. The solid line represents a fit of the data to the three-state model shown in Fig. 5b. The dashed lines indicate the hypothetical chevron plot for each of the two consecutive transition states (TS1 and TS2, cf. Fig. 5b). Data were taken from [42].

ships in many other apparent two-state folders (Sánchez and Kiefhaber, submitted). This argues for the generality of free energy landscapes with multiple sequential transition states in apparent two-state folding and shows that the analysis of

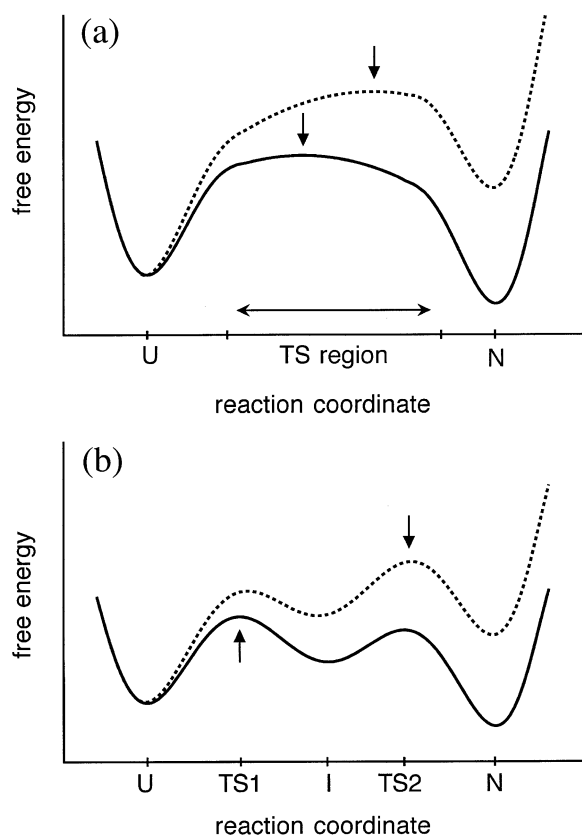


Fig. 5. Different possible origins for a denaturant-induced movement of a protein folding transition state along the reaction coordinate. The lines represent two-dimensional free energy landscapes at a low (—) and at a higher denaturant concentration (····). The arrows indicate the point on the reaction coordinate with the highest free energy. (a) Movement along a broad transition state region with a continuum of states with similar free energy in accordance with Hammond behavior. (b) Sequential transition states with a metastable high energy intermediate. If the intermediate (I) is less than stable than both the native state and the unfolded state under all conditions apparent two-state folding will be observed.

non-linear activation free energy relationships can be used to characterize the mechanism and the properties of free energy barriers in protein folding.

### 5. Cross-interaction parameters in protein folding.

Cross-interaction parameters have rarely been used to characterize protein folding reactions. For

tendamistat folding the denaturant dependence of the folding reaction was measured at different pressures [43]. This allows the calculation of the pressure/denaturant cross-interaction parameter ( $p_{DP}$ ). Fig. 6 shows equilibrium transition curves and chevron plots at pressures between 20 and 1000 bar. Increasing pressure destabilizes tendamistat leading to a shift of the GdmCl-induced unfolding transition to lower GdmCl concentrations (Fig. 6a) and indicating that the native state has a larger volume than the unfolded state. The

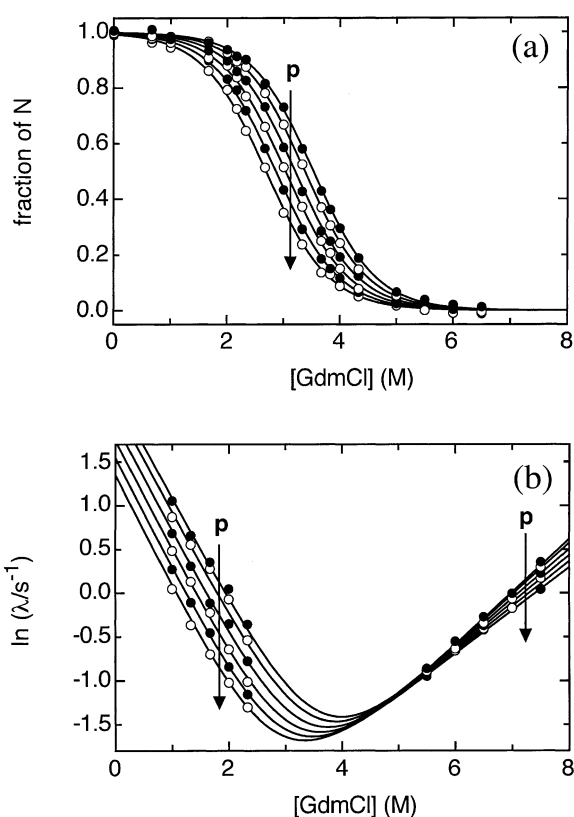


Fig. 6. Effect of pressure and denaturant on (a) the stability and (b) the apparent folding rate constant ( $\lambda$ ) of wild-type tendamistat at pH 2. The lines represent a global fit of the GdmCl and pressure dependence of the equilibrium constant ( $K_{eq}$ ) and the microscopic rate constants  $k_u$  and  $k_f$ , according to the two-state model. The arrows indicate the effect of increasing pressure at constant denaturant concentration on the fraction of native molecules (a) and on the apparent folding rate constant (b). The data sets were taken at 20, 200, 400, 600, 800 and 1000 bar. Data and fits were taken from [43].

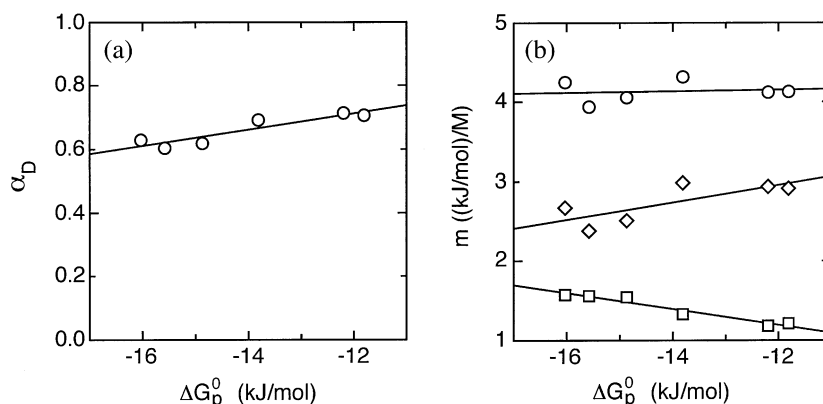


Fig. 7. Effect of  $\Delta G_p^0$  on  $\alpha_D$  (a) and on  $m_{eq}$  (○)  $m_f$  (◇) and  $m_u$  (□) (b) for the pressure/denaturant perturbation of tendamistat folding. The linear fits (solid lines) give values of  $p_{DP} = \partial\alpha_D/\partial\Delta G_p^0 = 0.025 \pm 0.006$  mol/kJ (a) and  $\partial m_u/\partial\Delta G_p^0 = -0.10 \pm 0.01$  M<sup>-1</sup>,  $\partial m_f/\partial\Delta G_p^0 = 0.11 \pm 0.05$  M<sup>-1</sup> and  $\partial m_{eq}/\partial\Delta G_p^0 = 0.01 \pm 0.04$  M<sup>-1</sup> (b). The data are taken from individual fits of the Chevron plots shown in Fig. 6b at different pressures and were re-analyzed according to Eq. (15).

reaction volume was found to be independent of the GdmCl concentration and the  $m_{eq}$ -value independent of pressure, which shows that the ground states are not effected by the perturbations ( $\partial m_{eq}/\partial p = \partial V^0/\partial[\text{GdmCl}] = 0$ ). The  $m_f$  and  $m_u$ -values, in contrast, are pressure dependent (Fig. 6b). Increasing pressure leads to a more native like transition state as judged by its solvent accessible surface area (increased  $m_f$ -value, decreased  $m_u$  value). As postulated from the Gibbs fundamental equation (Eq. (4)) this transition state movement is also observed as a denaturant-dependent increase in the volume of the transition state. The data in Fig. 6a,b were fitted globally with  $\partial m_f/\partial p = \partial\Delta V_f^{0\dagger}/\partial[\text{GdmCl}] = 2.5 \pm 0.6$  (cm<sup>3</sup>/mol)/M [43]. Interestingly, the volume of the transition state exceeds the volume of the native state at high denaturant concentrations as indicated by a decrease in the unfolding rate constant with increasing pressure above 5 M GdmCl (Fig. 6b). This scenario is not treated in the original Leffler postulate that the properties of the transition state are between those of the reactants and the products. The denaturant/pressure-induced non-linear activation free energy relationships in tendamistat indicate a transition state movement towards a less solvent-exposed structure when the protein is destabilized [43]. The

data were used to calculate the denaturant/pressure cross-interaction parameter

$$p_{DP} = \frac{\partial\alpha_D}{\partial\Delta G_p^0} = \frac{\partial\alpha_p}{\partial\Delta G_D^0} = p_{pD} \quad (15)$$

Fig. 7 shows the effect of on the  $\alpha_D$ -value for the denaturant-pressure dependent folding data shown in Fig. 6. The  $\alpha_D$ -value increases significantly with decreasing stability indicating a positive  $p_{pD}$ -value (Fig. 7a). Fig. 7b shows that the effect of is only observed in the kinetic  $m$ -values while  $m_{eq}$  is unchanged due to compensating changes in  $m_f$  and  $m_u$ . This indicates a true denaturant/pressure-induced transition state movement. It is not clear, however, whether a single transition state changes its structure according to Hammond behavior or whether a switch between two barriers on a sequential pathway occurs as observed in  $\alpha_D$  analysis of the C45A/C73A tendamistat variant (Figs. 4 and 5b).

For wild-type tendamistat [44] and the C45A/C73A variant [42] the temperature-denaturant cross-interactions parameters ( $p_{DT}$ ) were measured. For both transition states (TS1 and TS2 in Fig. 5)  $p_{DT}$  was zero indicating narrow barriers.

The popularity of the  $\phi_f$ -value analysis of folding transition states provides a wealth of data on  $\alpha_D$ ,  $\Delta G^0$  and  $\Delta G_{f,u}^{0\dagger}$  for many variants of several



proteins. This allows the calculation of denaturant/structure cross-interaction parameters ( $p_{DS}$ ) to analyze the effect of a change in protein stability ( $\Delta G^0$ ) caused by a structural change on the  $\alpha_D$ -value, i.e. on the relative change in solvent accessible surface area in the transition state.

$$p_{DS} = \frac{\partial \alpha_D}{\partial \Delta G_S^0} = \frac{\partial \phi_f}{\partial \Delta G_D^0} = p_{SD} \quad (16)$$

For several proteins non-zero  $p_{DS}$ -values were reported in literature which would indicate broad transition barriers with a continuum of energetically similar states [37,39,40,45]. However, one has to distinguish genuine Hammond behavior

from apparent transition state movements caused by ground state effects (see above and Fig. 3). In the following we will present a way to analyze data from mutational studies that allows a distinction between the different possible origins of the observed transition state movements.

## 6. Ground state effects vs. Hammond behavior

A change in the structure of one of the ground states of a reaction changes the ‘length’ of the reaction coordinate, which can lead to an apparent movement of the position of the transition state without a change in its structure (Fig. 3). Genuine

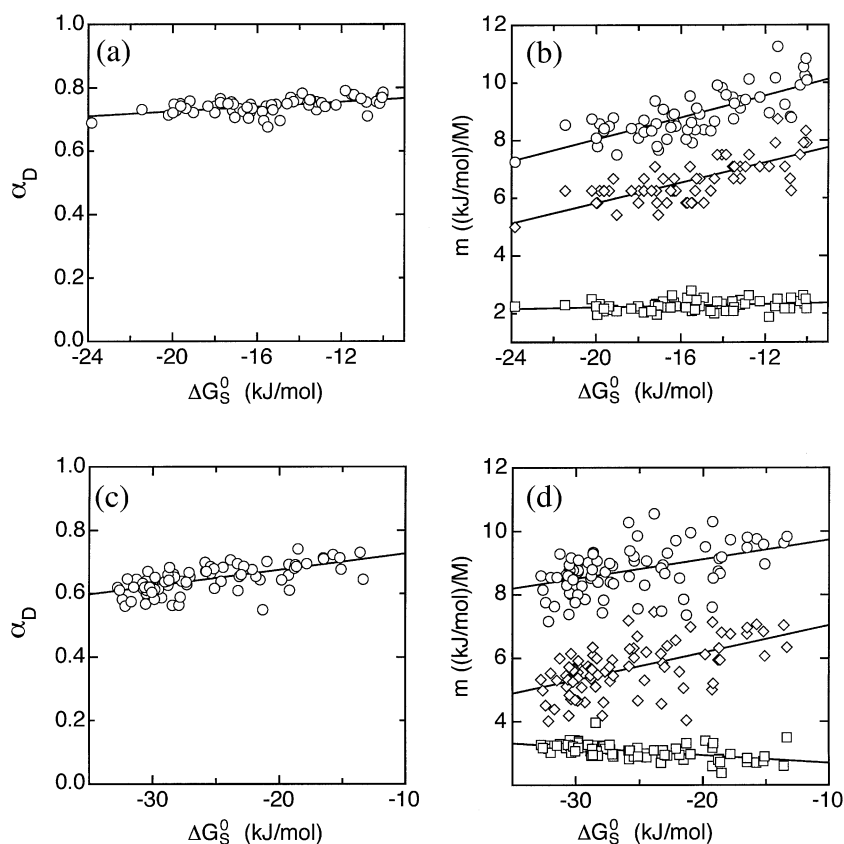


Fig. 8. Effect of  $\Delta G_S^0$  on  $\alpha_D$  (a, c) and on  $m_{eq}$  ( $\circ$ ),  $m_f$  ( $\diamond$ ) and  $m_u$  ( $\square$ , b, d) for the mutation/denaturant perturbation of protein L (a, b) and CI2 (c, d). The linear fits (solid lines) give values of  $p_{DS} = \partial \alpha_D / \partial \Delta G_S^0 = 3.8 \pm 0.8 \times 10^{-3}$  mol/kJ (a),  $\partial m_u / \partial \Delta G_S^0 = 0.01 \pm 0.01$  M $^{-1}$ ,  $\partial m_f / \partial \Delta G_S^0 = 0.18 \pm 0.02$  M $^{-1}$  and  $\partial m_{eq} / \partial \Delta G_S^0 = 0.19 \pm 0.02$  M $^{-1}$  (b) for protein L and of  $p_{DS} = \partial \alpha_D / \partial \Delta G_S^0 = 5.1 \pm 0.7 \times 10^{-3}$  mol/kJ (c),  $\partial m_u / \partial \Delta G_S^0 = -0.024 \pm 0.004$  M $^{-1}$ ,  $\partial m_f / \partial \Delta G_S^0 = 0.09 \pm 0.01$  M $^{-1}$  and  $\partial m_{eq} / \partial \Delta G_S^0 = 0.06 \pm 0.01$  M $^{-1}$  (d) for CI2. The data are taken from ref. [59] for protein L and from ref. [23] for CI2 and were re-analyzed according to Eq. (16). Only mutants with  $\Delta G^0 < -10$  kJ/mol were analyzed due to the larger errors in the analysis of the more unstable variants.

Hammond behavior moves the transition state away from one ground state and closer to the other one (Fig. 3b). Applied to denaturant-dependent folding reactions this will result in compensating effects on the  $m_f$ - and  $m_u$ -values and a constant  $m_{eq}$ -value, as observed for the pressure/denaturant cross-interaction parameter in tendamistat (Figs. 6 and 7). The discrimination between ground state effects and real transition state movements therefore requires the analysis of the effect of a change in  $\Delta G^0$  on both the equilibrium and the kinetic  $m$ -values. Fig. 8 shows the effect of a change in  $\Delta G^0$  induced by mutations  $\partial\Delta G_S^0$  on the  $\alpha_D$ -values (panels A and C) and on the  $m_{eq}$ -,  $m_f$ - and  $m_u$ -values for protein L (Fig. 8 a,b) and CI2 (Fig. 8c,d). Both proteins show an increasing  $\alpha_D$ -value with decreasing protein stability in accordance with Hammond behavior (Fig. 8a,c). However, the origins for the changing  $\alpha_D$ -values are different in the two proteins. In protein L the  $m_{eq}$ -value changes significantly upon mutation indicating structural changes it at least one of the ground states. The value of  $m_f$  changes by the same amount as  $m_{eq}$  while  $m_u$  is essentially independent of protein stability (Fig. 8b). This indicates that the structure of the transition state does not move relative to the structure of the native state (cf. Fig. 3). The increased in  $m_{eq}$ - and  $m_f$ -values point at the disruption of interactions in the unfolded state upon mutation, which leads to a less compact unfolded state. These results show that the apparent shift in the position of the transition state along the reaction coordinate seen for protein L is a ground state effect on the unfolded state rather than Hammond behaviour. In CI2 a change in stability indeed results in opposing effects on  $m_f$  and  $m_u$  accompanied by a significant change in the  $m_{eq}$ -values. The small change in  $m_u$  indicates transition state movement in addition to ground state effects. Structural changes in the unfolded state can be rationalized in the light of the results on the structure of unfolded proteins. Recently, several high resolution NMR studies have shown that both native-like and non-native-like interactions are present in unfolded states of several proteins [46–59] including protein L [57]. These interactions

may be disrupted by mutations and thus lead to changes in the  $m_{eq}$ -values [58].

The results on protein L stress the need for an analysis of the  $m_{eq}$ -,  $m_f$ - and  $m_u$ -values to distinguish genuine Hammond behavior from ground state effects. Accordingly, a ground state effect can also be mistaken for transition state movement if the effect of a change in only one of the activation free energies on  $\alpha_D$  is considered, which is commonly done in analysis of experimental data [7].

## 7. Conclusions

Self-interaction and cross-interaction parameters are useful tools to detect non-linear rate-equilibrium free energy relationships in protein folding. They can give valuable information on the shape of free energy barriers and thus on the mechanism of protein folding. However, non-linear free energy relationships in protein folding can have different molecular origins like a change in the rate limiting step of the folding reaction (Fig. 4b) or Hammond behaviour (Fig. 8 c,d). As in simple organic reactions structural changes in proteins (e.g. a point mutation) can significantly change the structure of the native state and/or of the unfolded state leading to ground state effects. These effects can, however, be distinguished from genuine transition state movement if the position of the transition state relative to both the native state and the unfolded state is determined.

## Acknowledgments

This work was supported by a grant from the Swiss National Science Foundation.

## References

- [1] J.E. Leffler, *Science* 117 (1953) 340–341.
- [2] C.D. Johnson, *Chem. Rev.* 75 (1975) 755–765.
- [3] W.P. Jencks, *Chem. Rev.* 85 (1985) 511–527.
- [4] G.S. Hammond, *J. Am. Chem. Soc.* 77 (1955) 334–338.
- [5] E.R. Thornton, *J. Am. Chem. Soc.* 89 (1967) 2915–2927.
- [6] P. Müller, *Pure Appl. Chem.* 66 (1994) 1077–1184.
- [7] D. Farcasiu, *J. Chem. Ed.* 52 (1975) 76–79.
- [8] D.A. Jencks, W.P. Jencks, *J. Am. Chem. Soc.* 99 (1977) 7948–7960.

- [9] M.G. Evans, M. Polanyi, *Trans. Faraday Soc.* 31 (1935) 875–885.
- [10] H. Eyring, *J. Chem. Phys.* 3 (1935) 107–115.
- [11] M. Planck, *Ann. Phys. Chem.* 32 (1887) 462–503.
- [12] M. Jäger, H. Nguyen, J.C. Crane, J.W. Kelly, M. Gruebele, *J. Mol. Biol.* 311 (2001) 373–393.
- [13] F.M. Pohl, *FEBS Lett.* 65 (1976) 293–296.
- [14] B.L. Chen, W.A. Baase, J.A. Schellman, *Biochemistry* 28 (1989) 691–699.
- [15] C.N. Pace, *Meth. Enzymol.* 131 (1986) 266–280.
- [16] J.K. Myers, C.N. Pace, J.M. Scholtz, *Protein Sci.* 4 (1995) 2138–2148.
- [17] C. Tanford, *Adv. Prot. Chem.* 24 (1970) 1–95.
- [18] K.W. Plaxco, D. Baker, *Proc. Natl. Acad. Sci. USA* 95 (1998) 13591–13596.
- [19] S. Sato, C.J. Sayid, D.P. Raleigh, *Protein Sci.* 9 (2000) 1601–1603.
- [20] D. Perl, M. Jacob, M. Bánó, M. Stupák, M. Antalík, F.X. Schmid, *Biophys. Chem.* 96 (2002) 173–190.
- [21] C.R. Matthews, *Meth. Enzymol.* 154 (1987) 498–511.
- [22] A.R. Fersht, A. Matouschek, L. Serrano, *J. Mol. Biol.* 224 (1992) 771–782.
- [23] L.S. Itzhaki, D.E. Otzen, A.R. Fersht, *J. Mol. Biol.* 254 (1995) 260–288.
- [24] C. Grosman, M. Zhou, A. Auerbach, *Nature* 403 (2000) 773–776.
- [25] Y.K. Mok, E.L. Eliseeva, A.R. Davidson, J.D. Forman-Kay, *J. Mol. Biol.* 307 (2001) 913–928.
- [26] A.R. Fersht, L.S. Itzhaki, N.F. elMasry, J.M. Matthews, D.E. Otzen, *Proc. Natl. Acad. Sci. USA* 91 (1994) 10426–10429.
- [27] B.A. Krantz, L.B. Moran, A. Kentsis, T.R. Sosnick, *Nat. Struct. Biol.* 7 (2000) 62–71.
- [28] K. Kuwajima, M. Mitani, S. Sugai, *J. Mol. Biol.* 206 (1989) 547–561.
- [29] J. Sancho, E.M. Meiering, A.R. Fersht, *J. Mol. Biol.* 221 (1991) 1007–1014.
- [30] Y.J. Tan, M. Oliveberg, A.R. Fersht, *J. Mol. Biol.* 264 (1996) 377–389.
- [31] B.A. Krantz, T.R. Sosnick, *Nat. Struct. Biol.* 8 (2001) 1042–1047.
- [32] G.I. Makhatadze, P.L. Privalov, *Adv. Prot. Chem.* 47 (1995) 307–425.
- [33] D.J. Wales, *Science* 293 (2001) 2067–2070.
- [34] A. Ikai, W.W. Fish, C. Tanford, *J. Mol. Biol.* 73 (1973) 165–184.
- [35] S.E. Jackson, A.R. Fersht, *Biochemistry* 30 (1991) 10428–10435.
- [36] N. Schönbrunner, K.-P. Koller, T. Kiefhaber, *J. Mol. Biol.* 268 (1997) 526–538.
- [37] A. Matouschek, A.R. Fersht, *Proc. Natl. Acad. Sci. USA* 90 (1993) 7814–7818.
- [38] J.M. Matthews, A.R. Fersht, *Biochemistry* 34 (1995) 6805–6814.
- [39] A. Matouschek, D.E. Otzen, L. Itzhaki, S.E. Jackson, A.R. Fersht, *Biochemistry* 34 (1995) 13656–13662.
- [40] M. Oliveberg, Y.-J. Tan, M. Silow, A.R. Fersht, *J. Mol. Biol.* 277 (1998) 933–943.
- [41] P.A. Dalby, M. Oliveberg, A.R. Fersht, *Biochemistry* 37 (1998) 4674–4679.
- [42] A. Bachmann, T. Kiefhaber, *J. Mol. Biol.* 306 (2001) 375–386.
- [43] G. Pappenberger, C. Saudan, M. Becker, A.E. Merbach, T. Kiefhaber, *Proc. Natl. Acad. Sci. USA* 97 (2000) 17–22.
- [44] N. Schönbrunner, G. Pappenberger, M. Scharf, J. Engels, T. Kiefhaber, *Biochemistry* 36 (1997) 9057–9065.
- [45] M. Silow, M. Oliveberg, *Biochemistry* 36 (1997) 7633–7637.
- [46] P.A. Evans, K.D. Topping, D.N. Woolfson, C.M. Dobson, *Proteins* 9 (1991) 248–266.
- [47] D. Neri, M. Billeter, G. Wider, K. Wüthrich, *Science* 257 (1992) 1559–1563.
- [48] T.M. Logan, Y. Theriault, S.W. Fesik, *J. Mol. Biol.* 236 (1994) 637–648.
- [49] C.K. Smith, Z.M. Bu, K.S. Anderson, J.M. Sturtevant, D.M. Engelman, L. Regan, *Protein Sci.* 5 (1996) 2009–2019.
- [50] N. Sari, P. Alexander, P.N. Bryan, J. Orban, *Biochemistry* 39 (2000) 965–977.
- [51] K.B. Wong, J. Clarke, C.J. Bond, J.L. Neira, S.M. Freund, A.R. Fersht, V. Daggett, *J. Mol. Biol.* 296 (2000) 1257–1282.
- [52] K. Teilum, B.B. Kragelund, J. Knudsen, F.M. Poulsen, *J. Mol. Biol.* 301 (2000) 1307–1314.
- [53] T. Kortemme, M.J. Kelly, L.E. Kay, J.D. Forman-Kay, L. Serrano, *J. Mol. Biol.* 297 (2000) 1217–1229.
- [54] P. Garcia, L. Serrano, D. Durand, M. Rico, M. Bruix, *Protein Sci.* 10 (2001) 1100–1112.
- [55] W.Y. Choy, J.D. Forman-Kay, *J. Mol. Biol.* 308 (2001) 1011–1032.
- [56] S.L. Kazmirski, K.B. Wong, S.M. Freund, Y.J. Tan, A.R. Fersht, V. Daggett, *Proc. Natl. Acad. Sci. USA* 98 (2001) 4349–4354.
- [57] Q. Yi, M.L. Scalley-Kim, E.J. Alm, D. Baker, *J. Mol. Biol.* 299 (2000) 1341–1351.
- [58] J. Klein-Seetharaman, M. Oikawa, S.B. Grimshaw, et al., *Science* 295 (2002) 1719–1722.
- [59] D.E. Kim, C. Fisher, D. Baker, *J. Mol. Biol.* 298 (2000) 971–984.